

See discussions, stats, and author profiles for this publication at: <https://www.researchgate.net/publication/357093167>

# Observing the suppression of individual aversive memories from conscious awareness

Preprint · December 2021

CITATIONS

0

READS

107

5 authors, including:



**Xuanyi Lin**

The University of Hong Kong

7 PUBLICATIONS 10 CITATIONS

[SEE PROFILE](#)



**Danni Chen**

The University of Hong Kong

8 PUBLICATIONS 18 CITATIONS

[SEE PROFILE](#)



**Ziqing Yao**

The University of Hong Kong

8 PUBLICATIONS 43 CITATIONS

[SEE PROFILE](#)



**Michael C Anderson**

University of Cambridge

102 PUBLICATIONS 10,189 CITATIONS

[SEE PROFILE](#)

Some of the authors of this publication are also working on these related projects:



Understanding endogenous emotions [View project](#)



Brain-to-brain coupling underlying social interaction (cooperation and communication) [View project](#)

# Observing the suppression of individual aversive memories from conscious awareness

Xuanyi Lin<sup>1</sup>, Danni Chen<sup>1</sup>, Ziqing Yao<sup>1</sup>, Michael C. Anderson<sup>2, CA</sup>, and Xiaoqing Hu<sup>1, CA</sup>

<sup>1</sup>Department of Psychology, The State Key Laboratory of Brain and Cognitive Sciences, University of Hong Kong; <sup>2</sup>MRC Cognition & Brain Sciences Unit, Behavioural and Clinical Neuroscience Institute, University of Cambridge

Correspondences: xiaqinghu@hku.hk; michael.anderson@mrc-cbu.cam.ac.uk

1 **When reminded of an unpleasant experience, people often try to ex-**  
2 **clude the unwanted memory from awareness, a process known as**  
3 **retrieval suppression. Despite the importance of this form of mental**  
4 **control to mental health, the ability to track, in real time, individual**  
5 **memories as they are suppressed remains elusive. Here we used**  
6 **multivariate decoding on EEG data to track how suppression unfolds**  
7 **in time and to reveal its impact on cortical patterns related to indi-**  
8 **vidual memories. We presented reminders to aversive scenes and**  
9 **asked people to either suppress or to retrieve the scene. During**  
10 **suppression, mid-frontal theta power within the first 500 ms distin-**  
11 **guished suppression from passive viewing of the reminder, indicating**  
12 **that suppression rapidly recruited control. During retrieval, we could**  
13 **discern EEG cortical patterns relating to individual memories-initially,**  
14 **based on theta-driven, visual perception of the reminders (0-500 ms)**  
15 **and later, based on alpha-driven, reinstatement of the aversive scene**  
16 **(500-3000 ms). Critically, suppressing retrieval weakened (during 420-**  
17 **600 ms) and eventually abolished item-specific cortical patterns, a**  
18 **robust effect that persisted until the reminder disappeared (1200-3000**  
19 **ms). Actively suppressing item-specific cortical patterns, both during**  
20 **an early (300-680 ms) window and during sustained control, predicted**  
21 **later episodic forgetting. Thus, both rapid and sustained control con-**  
22 **tribute to abolishing cortical patterns of individual memories, limiting**  
23 **awareness, and precipitating later forgetting. These findings reveal**  
24 **how suppression of individual memories from awareness unfolds in**  
25 **time, presenting a precise chronometry of this process.**

Retrieval Suppression | Forgetting | Memory | EEG | MVPA

## 1 Introduction

2 Following an upsetting event, memories of the experience often  
3 come to mind uninvitedly. Even seemingly innocuous  
4 reminders can bring us back to the traumatic scene in the  
5 blink of an eye, triggering intrusive memories and distress.  
6 When this happens, people often recruit inhibitory control to  
7 terminate unwelcome retrieval, a process known as retrieval  
8 suppression (Anderson & Hulbert, 2020; Küpper et al., 2014).  
9 An ability to control aversive memories and to keep them  
10 out of awareness can promote resilience and safeguard mental  
11 well-being, especially in the aftermath of trauma (Anderson  
12 & Hanslmayr, 2014; Catarino et al., 2015; Engen & Ander-  
13 son, 2018; Hu et al., 2017; Mary et al., 2020). Despite the  
14 fundamental importance of this process, much remains un-  
15 known about its basic mechanisms. Indeed, no study has  
16 yet observed individual memories as they are suppressed, a  
17 pre-requisite to tracking the dynamics of memory control.  
18 Observing suppression unfold in real time is fundamental to  
19 advance neurobiological models of memory control, and to  
20 inform novel interventions that may aid people in forgetting  
21 unwanted memories.

22 Neuroimaging research suggests that during retrieval sup-

pression, when a person sees a reminder to an unwanted  
memory, the prefrontal cortex exerts inhibitory control over  
the hippocampus and its adjacent medial temporal lobe struc-  
tures to stop retrieval (Anderson et al., 2004; Depue et al.,  
2007). Furthermore, inhibitory control down-regulates activity  
in content-specific neocortical areas implicated in the encoding  
of the original memory (Benoit et al., 2015; Depue et al., 2007;  
Gagnepain et al., 2014, 2017; Hu et al., 2017; Mary et al.,  
2020). Given its limited temporal resolution, however, func-  
tional magnetic resonance imaging does not permit a detailed  
account of the temporal dynamics underlying the suppression  
of individual memory representations.

Conversely, although EEGs have the temporal resolution  
needed to track the online dynamics of retrieval suppression  
(Bergström et al., 2009; Hellerstedt et al., 2016; Hu et al.,  
2015; Zhang et al., 2016), its poor spatial resolution has his-  
torically rendered it difficult to isolate individual memories  
as they are suppressed. However, advances in multivariate  
pattern analysis have allowed researchers to exploit distinctive  
EEG scalp distributions to identify specific memory repre-  
sentations (Bae & Luck, 2018; Treder et al., 2021; Wolff et  
al., 2017). Here, leveraging EEGs' temporal resolution, and  
multivariate decoding analyses, we sought to isolate cortical  
EEG patterns unique to individual memories, and to observe  
suppression abolishing such patterns in real time. For this  
purpose, we adapted the think/no-think paradigm to require  
our participants to voluntarily retrieve or to suppress aver-  
sive scenes when confronting reminders (Anderson & Green,  
2001; Depue et al., 2007; Küpper et al., 2014). To track the  
temporal dynamics of retrieval suppression, we took a two-  
step approach to our EEG analysis. First, we used decoding  
to determine how and when suppression differed, in general,  
from retrieval; thus, using data from all EEG sensors, we  
applied multivariate EEG analysis to compare retrieval and  
retrieval-suppression manipulations to a perceptual baseline  
condition, in which neither retrieval nor suppression had oc-  
curred. Pairwise condition-level decoding should reveal neural  
dynamics of retrieval and retrieval suppression, relative to the  
no-retrieval baseline. We focused on the role of frontal theta  
within the first 500 ms, given frontal theta power increase  
has been related to inhibitory control processes (Anderson &  
Hulbert, 2020; Cavanagh & Frank, 2014; Crespo-García et al.,  
2021; Nigbur et al., 2011).

We next used MVPA within each condition to isolate item-  
specific cortical EEG patterns and to examine their develop-  
ment over time in relation to the suppression process. We hy-  
pothesized successful suppression and forgetting of unwanted  
memories involves two key requirements. First, inhibitory  
control needs to act rapidly to truncate retrieval before the  
reminder elicits episodic recollection, reinstating the aversive

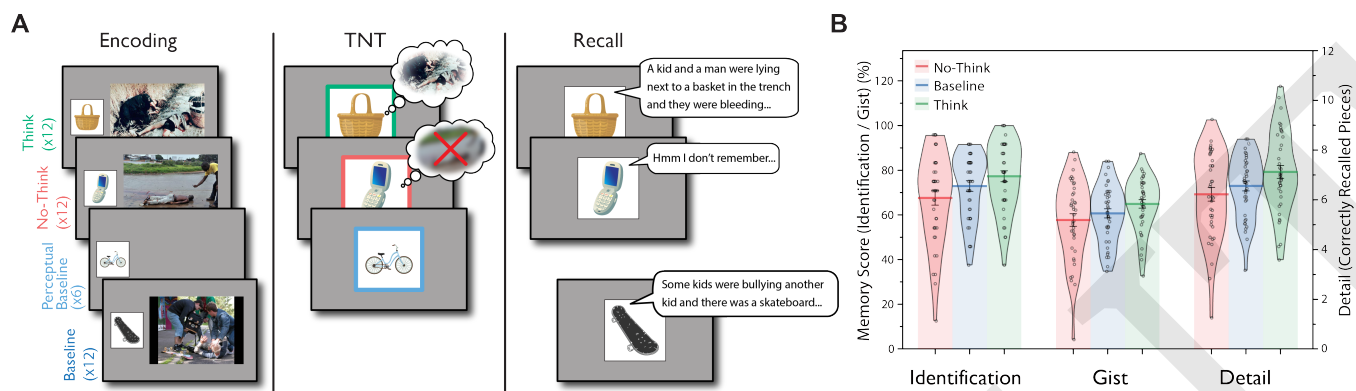


**Fig. 1.** Experimental Procedure and Suppression-Induced Forgetting. (A) The emotional Think/No-Think task (eTNT) included three phases. 1) Encoding: Participants first learned object-aversive scene stimulus pairings; and they also viewed some objects without any paired scene (i.e., Perceptual Baseline); 2) Think/No-Think (TNT) task: Participants either retrieved (Think) or suppressed the retrieval (No-Think) of negative scene memories. Participants were also presented with Perceptual Baseline trials without any retrieval; Think, No-Think, and Perceptual Baseline instructions were cued by a green, red, or blue colored box respectively, surrounding the cue object; 3) Recall: Participants viewed object cues and verbally described their associated scenes. (B) Suppression-Induced Forgetting on Identification, Gist and Detail measures from the Recall test. Suppression-induced forgetting can be seen in the lower recall of No-Think than Baseline items ( $n = 40$ ).

73 scene. Second, inhibition must be sustained over time and ex- 114  
 74 punge intruding memories from awareness, abolishing residual 115  
 75 cortical reinstatements. The initial truncation of retrieval must  
 76 proceed very rapidly; research on the time course of memory  
 77 retrieval reveals a chronometry with multiple stages. Upon  
 78 visually perceiving a memory cue, a cue-to-memory conversion  
 79 process is thought to occur within 500 ms, along the occipital-  
 80 temporal cortex pathway. Outputs of this process are thought  
 81 to arrive in the hippocampus, initiating pattern completion  
 82 at around 500 ms. Pattern completion is thought to then  
 83 drive cortical reinstatement of the associated target memory  
 84 during the 500-1500 ms window, at least for simple laboratory  
 85 materials (Staresina et al., 2019; Staresina & Wimber, 2019;  
 86 Treder et al., 2021; Yaffe et al., 2014).

87 Based on these findings, we hypothesized that countering  
 88 the emergence of item-specific cortical patterns would involve  
 89 inhibitory control to target processes in the cue-to-memory  
 90 conversion window (at around 500 ms) and also in the cortical  
 91 reinstatement window (500-1500 ms). To understand how sup-  
 92 pression modulates item-specific activity, we further examined  
 93 4-8 Hz theta activity during the early 0-500 ms time window,  
 94 given the roles of theta in sensory intake and feedforward  
 95 information flow originating from the sensory cortex (Bastos  
 96 et al., 2015; Colgin, 2013). To track reinstatement, we focused  
 97 on 9-12 Hz alpha activity in the 500-1500 ms window, given  
 98 alpha activity's role in working memory maintenance and re-  
 99 instatement (Fellner et al., 2020; Jensen et al., 2002). By  
 100 comparing how item-specific cortical patterns unfold over time  
 101 between the retrieval and the retrieval suppression conditions,  
 102 we gain a window into the timeline for how inhibitory control  
 103 affects the recollection of individual memories.

104 We found that suppressing retrieval enhanced early theta  
 105 control and began to attenuate item-specific cortical patterns  
 106 within the first 500 ms, likely disrupting the perception-to-  
 107 memory conversion processes. Critically, retrieval suppression  
 108 weakened and ultimately abolished item-specific cortical pat-  
 109 terns during the 500-1500 ms memory reinstatement window in  
 110 a sustained manner. These results were especially pronounced  
 111 among participants who successfully forgot the unpleasant  
 112 scenes that they suppressed; in contrast, less successful for-  
 113 getting was associated with insufficient mobilization of early

theta control mechanisms, and relapse of cortical patterns for  
 unwelcome content during the full suppression window.

## 116 Results

117 **Suppressing Retrieval Induces Forgetting of Emotional Mem-**  
 118 **ories.** Following the emotional Think/No-Think (TNT) task,  
 119 participants completed a cued recall test during which they  
 120 verbally described the aversive scene that they thought was  
 121 linked to each of the cue objects. We coded and scored ver-  
 122 bal descriptions on *Identification*, *Gist* and *Detail* (see Meth-  
 123 ods). Each of these three scores was submitted to a one-way  
 124 repeated-measure (Think, No-Think and Baseline) analysis  
 125 of variance (ANOVA). Results showed a significant condition  
 126 effect on *Identification*  $F(1.87,72.93) = 7.35, p = .002$ ; *Detail*  
 127  $F(1.93,75.2) = 13.79, p < .001$  and *Gist*  $F(1.92,74.95) =$   
 128  $6.22, p = .004$ . Planned contrasts comparing Baseline and  
 129 No-Think conditions confirmed that participants showed sig-  
 130 nificant suppression-induced forgetting on *Identification*,  $t(39)$   
 131  $= -2.07, p = .045, dz = 0.33$ , and *Details*,  $t(39) = -2.16, p =$   
 132  $.037, dz = 0.34$ , whereas the forgetting effect on *Gist* was not  
 133 significant  $t(39) = -1.58, p = .123, dz = 0.25$ , see Figure 1B).

134 **Stopping Retrieval is Distinct From Not-Retrieving.** We next  
 135 sought to identify EEG activity tied to stopping retrieval. To-  
 136 wards that end, we examined EEG activities that distinguished  
 137 No-Think, Think, and Perceptual Baseline (i.e., no-retrieval)  
 138 conditions. In the time domain, condition-level multivariate  
 139 decoding not only distinguished retrieval suppression from  
 140 voluntary retrieval (NT vs. T,  $p_{corrected} < .001$ , Figure 2C,  
 141 purple), but also from non-retrieval in our perceptual baseline  
 142 condition (NT vs. PB,  $p_{corrected} < .001$ , Figure 2C, red). These  
 143 differences imply that unique cognitive operations contributed  
 144 during retrieval suppression, consistent with the involvement  
 145 of an active stopping mechanism. Differences between No-  
 146 Think and Think conditions emerged as early as 140 ms and  
 147 persisted throughout the entire trial period until ~3000 ms. In  
 148 addition, we also could distinguish retrieval from non-retrieval  
 149 (T vs. PB,  $p_{corrected} < .001$ , Figure 2C, green). At least some  
 150 of the latter decoding difference arose from EEG correlates of  
 151 active retrieval processes during the Think condition: decoding

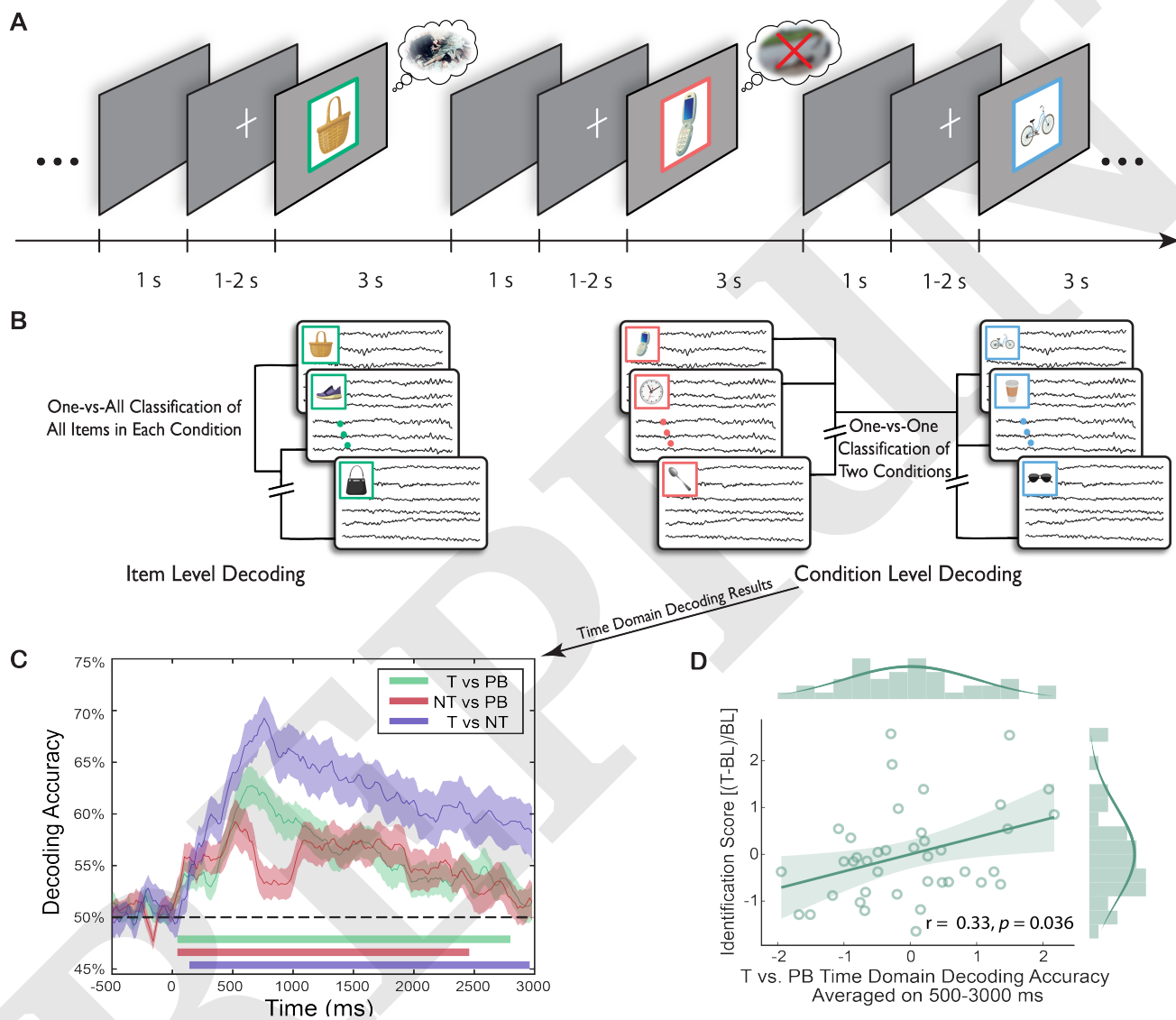


**Fig. 2.** Decoding Approaches Diagram and Condition-level Time-domain EEG Decoding Results. (A-B) An illustration of trial flow in the EEG-based eTNT task, and the logic of decoding analyses. (C) Condition-level decoding based on time domain EEGs revealed significant differences in all three pairwise comparisons. Colored lines along x-axis indicate significant clusters (permutation cluster corrected): No-Think vs Perceptual Baseline, 40-2460 ms,  $p_{\text{corrected}} < .001$ ; Think vs Perceptual Baseline, 40-2800 ms,  $p_{\text{corrected}} < .001$ ; Think vs No-Think, 140-2960 ms,  $p_{\text{corrected}} < .001$ . Shaded areas indicate standard errors of the mean (S.E.M). (D) Time domain Think vs. Perceptual Baseline decoding accuracies during the 500-3000 ms window was positively correlated with the enhancement of Think item recall on the final recall test, on the Identification score ((Think – Baseline)/Baseline), or the recall benefit, proportional to baseline).

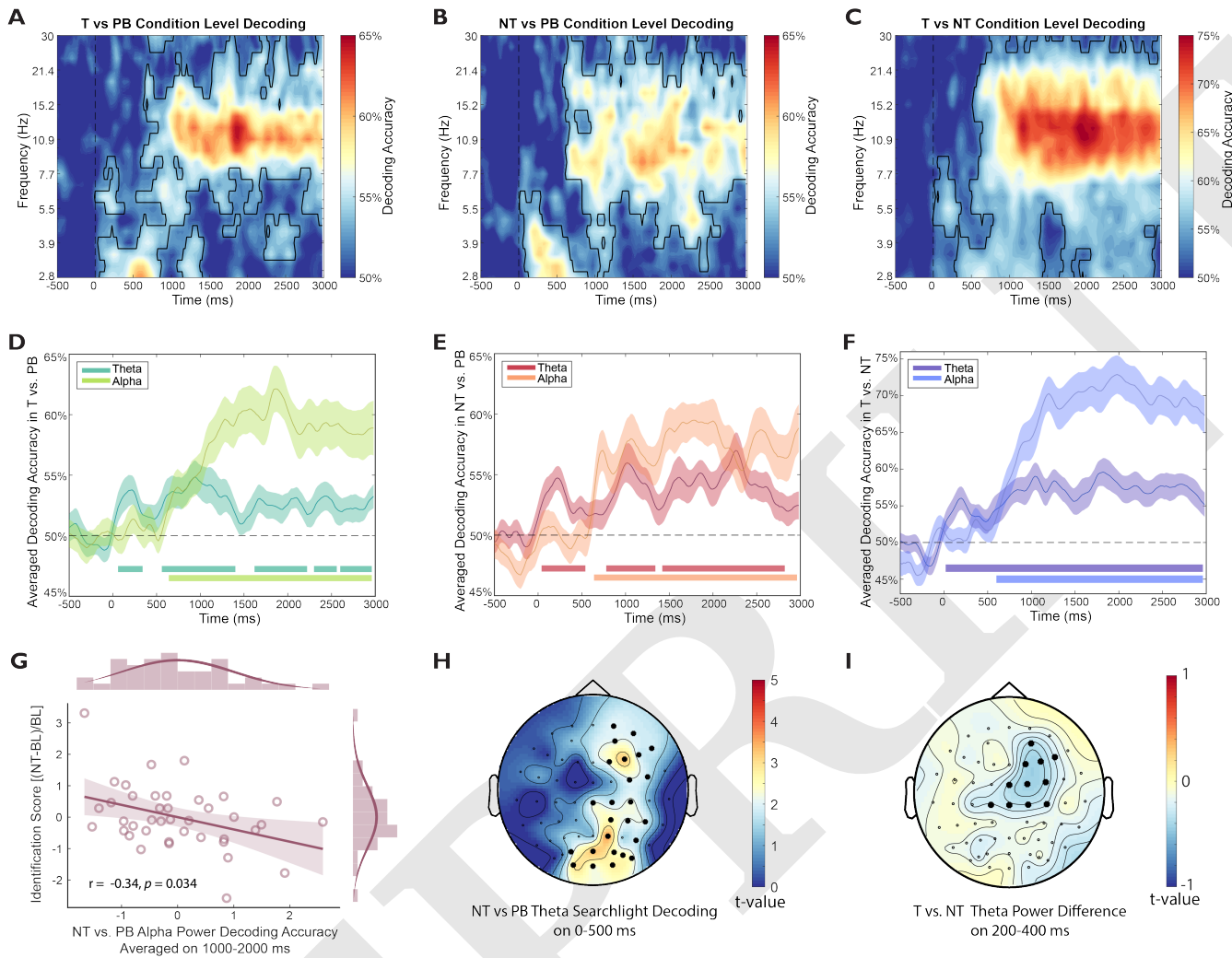


**Fig. 3.** The Condition-Level Time-Frequency Domain Decoding. (A-C) Condition-level time-frequency decoding results. Frequency is log scaled with the colorbar denoting decoding accuracy. Black outlined highlight significant clusters against chance level (both cluster and permutation  $\alpha$ s are set at 0.05). (D-F) Decoding accuracies in A-C are averaged on theta (4-8 Hz) and alpha (9-12 Hz) bands. Lines at the bottom denote significant clusters of averaged accuracy against chance level (50%) (G) The alpha-based No-Think vs. Perceptual Baseline decoding accuracies during 1,000-2,000 ms predicted later suppression-induced forgetting (i.e., higher decoding predicted a more negative score, or higher forgetting). (H) Theta power within 0-500 ms distinguished NT vs. PB over frontal and posterior brain regions in a channel searchlight decoding analysis. Significant electrodes were cluster corrected and are highlighted. (I) Theta power averaged from 200-400 ms was higher in NT than T. The increased theta power showed a frontal-central distribution. Significant electrodes were cluster corrected and are highlighted.

152 accuracies from 500-3000ms during the Think vs. Perceptual  
 153 Baseline analysis predicted retrieval-induced facilitation of  
 154 Think items in the Identification measure,  $r = 0.33, p = .036$ ;  
 155 and in the Detail measure,  $r = 0.33, p = .041$  (Figure 2D, also  
 156 see Figure S2A).

157 Retrieval suppression could also be distinguished from retrieval  
 158 and passive viewing based on time-frequency domain  
 159 EEGs. Between condition decoding revealed differences among  
 160 all pairwise comparisons (Figure 3A-F). Consistent with an  
 161 early, active control process associated with suppression, we  
 162 found, within the first 500 ms, significant NT vs. PB decoding  
 163 in 4-8 Hz theta activity over the frontal and posterior regions  
 164 (Figure 3E, 3H). This significant decoding continued throughout  
 165 the 3000 ms epoch. Theta power differences contributed to  
 166 this decoding: we found that during the 200-400 ms window,  
 167 retrieval suppression (vs. retrieval or passive viewing) led to  
 168 enhanced midline and right prefrontal theta power (NT > T,

169  $p_{corrected} = .007$ , Figure 3I; NT > PB,  $p_{corrected} = .002$ , Figure  
 170 S1G). After this early theta enhancement, suppression was  
 171 associated with reduced theta power from 500 to 3000 ms (NT  
 172 < T, theta:  $p_{corrected} = .004$ , NT < PB, theta:  $p_{corrected} <$   
 173  $.001$ ).

174 Retrieval suppression also could be distinguished based on  
 175 alpha activity, and such effects were enduring. Indeed, 9-12 Hz  
 176 alpha activity drove condition-level decoding performance between  
 177 500 to 3000 ms (Figure 3D-F) with retrieval suppression  
 178 reducing alpha (NT < T,  $p_{corrected} < .001$ ; NT < PB,  $p_{corrected}$   
 179  $= .002$ , Figure S1A-F). Based on a recent study indicating  
 180 that a 1000-2000 ms alpha power reduction may reflect reduced  
 181 rehearsal during memory control (Fellner et al., 2020),  
 182 we hypothesized that these alpha power reductions may have  
 183 behavioral implications. Strikingly, during the same 1000-2000  
 184 ms as in prior research, the ability to decode NT versus PB  
 185 based on alpha activity predicted suppression-induced forget-

186 ting on our *Identification* measure ( $r = -0.34$ ,  $p = .034$ , Figure  
187 3G, also see Figure S2B). This negative correlation suggests  
188 that reduced alpha power contributed to subsequent forget-  
189 ting of suppressed content. In contrast, whereas alpha-based  
190 NT vs. PB decoding accuracies predicted suppression-induced  
191 forgetting, the ability to decode T from PB based on alpha  
192 power predicted retrieval-induced facilitation for Think items,  
193 with the difference of these two correlations being significant  
194 (*Detail*:  $z = 2.06$ ,  $p = .039$ ; Figure S2C). Together, these  
195 findings suggest that increases in early theta power and reduc-  
196 tions in later theta/alpha power may be hallmarks of active  
197 suppression that make it qualitatively distinct from simply  
198 not-retrieving.

199 **Spatial Patterns in EEG Discern Individual Episodic Memo-**  
200 **ries During Retrieval.** Observing the suppression of individual  
201 memories requires an index sensitive to brain activity unique  
202 to each memory item so that the impact on suppression on  
203 that index may be tracked. We hypothesized that the spatio-  
204 temporal pattern of scalp-EEG as participants thought about  
205 each scene may contain information sufficient to distinguish  
206 that specific scene from all the others. To test this hypothe-  
207 sis, we performed a decoding analysis on scalp-EEG patterns  
208 during Think trials, during which participants actively rein-  
209 stated associated scenes. Consistent with our hypothesis,  
210 time-domain EEGs distinguished between individual scene  
211 memories across the entire 0-3000 ms window (Figure 4A,  
212  $p_{\text{corrected}} < .001$ ). In sharp contrast, for Perceptual Baseline  
213 trials, above-chance decoding of individual items arose only  
214 in the 0-500 ms (to be precise, 60-640 ms,  $p_{\text{corrected}} < .001$ ),  
215 but not in the 500-3000 ms window (Figure 4C). To directly  
216 compare item-level decoding between retrieval and PB, we  
217 repeated the analyses with 6 randomly sampled items from the  
218 Think condition, to match the item number in the Perceptual  
219 Baseline (see Methods). We found that Think trials showed  
220 higher item-level decoding accuracies than Perceptual Baseline  
221 trials during the 360-1180 ms ( $p_{\text{corrected}} < .001$ ) and 1220-1540  
222 ms window ( $p_{\text{corrected}} = .022$ , Figure 4K, purple lines).

223 Successful decoding of individual items in the early time  
224 window (0 – 360ms) likely reflects visual processing of unique  
225 object retrieval cues, which are present both for the object-  
226 scene pairs used in the Think condition, and in the single  
227 objects used in the PB condition. In the later 360-1540 ms  
228 time window, however, higher decoding during Think trials  
229 would need to be driven by an item-specific processing present  
230 in the Think condition but not in the PB condition. One  
231 possibility is that this later item-specific effect in the Think  
232 condition may reflect the reinstatement and maintenance of  
233 unique unpleasant scenes associated to the object cue, which  
234 may have gradually begun to emerge in awareness as they  
235 were recollected. Another possibility, however, is that item-  
236 level decoding in the Think condition may simply reflect more  
237 sustained attention to the unique object cues in that condition,  
238 relative to the PB condition, for which participants may have  
239 correctly concluded that retrieval was unnecessary.

240 To distinguish these possibilities, we examined brain regions  
241 giving rise to above-chance decoding during Think trials using  
242 searchlight decoding (see Methods). If greater decoding of  
243 individual items in the Think condition reflected sustained  
244 attention on object cues, successful decoding may be restricted  
245 to visual processing regions involved in object perception.  
246 Indeed, during the first 500 ms, occipital EEGs primarily

247 drove the significant decoding in general, consistent with a  
248 primary role of visual-perceptual cue processing (Figure 4D).  
249 In contrast, during the latter 500-3000 ms interval, significant  
250 decoding rested on a distributed set of regions implicated in  
251 memory retrieval such as the right prefrontal and parietal-  
252 occipital cortex (Figure 4E). This finding suggests that item-  
253 level decoding beyond the first 500 ms is not dominated by  
254 object cue attention, but rather by the reinstatement of the  
255 associated scene memories. Converging with this possibility,  
256 item-level decoding performance during the latter 500-3000  
257 ms time window predicted later performance on the Detail  
258 measure of scene memory ( $r = 0.34$ ,  $p = .034$ , Figure 4J),  
259 whereas decoding during the early 0-500 ms time window did  
260 not ( $r = 0.01$ ,  $p = .946$ ).

261 Unlike during Think trials, the same searchlight analysis  
262 during Perceptual Baseline trials showed that significant decod-  
263 ing in the 0-500ms window arose over a small cluster of  
264 occipital electrodes. The restriction of decoding success to  
265 occipital cortex suggests that classification hinged on visual  
266 object processing during that period (Figure 4H). After this  
267 initial window, the latter part of the trial from 500-3000 ms  
268 showed no significant decoding at any electrode (Figure 4I;  
269 similar searchlight results were obtained when using 0-360 and  
270 360-1540 ms windows, see Figure S3A).

271 In sum, during retrieval, time-resolved EEG patterns sug-  
272 gest a staged cued-recall process: during the 0-500 ms window,  
273 EEG patterns could discern perceived items over occipital  
274 regions; during 500-3000 ms, EEG patterns could distinguish  
275 among retrieved items over fronto-parietal-occipital regions.  
276 Furthermore, higher item-level decoding accuracies predicted  
277 better scene memory only in this latter, 500-3000 ms time  
278 window.

279 **Suppressing Retrieval Weakens and Abolishes Item-specific**  
280 **Cortical Patterns.** Having established that the retrieval of indi-  
281 vidual scene memories can be indexed and tracked, we next  
282 sought to use this index to determine how and when suppres-  
283 sion affected cortical patterns relating to individual memories.  
284 We therefore examined whether retrieval suppression modu-  
285 lated item-specific cortical EEG patterns.

286 We hypothesized that item-level decoding during No-Think  
287 trials would be possible initially, as participants focused their  
288 attention on the visually unique reminder cues, but that sup-  
289 pression would limit successful decoding throughout the re-  
290 mainder of the trial. Indeed, in the No-Think condition,  
291 item-level decoding accuracy was above chance initially, and  
292 remained so until 1160 ms ( $p_{\text{scorrected}} < .028$ ); decoding ac-  
293 curacy then dropped to chance-levels for the remainder of  
294 the 3000ms trial. Consistent with the Think and Perceptual  
295 Baseline analyses, we used a priori defined time windows from  
296 0-500 and 500-3000 ms to characterize the EEG scalp distribu-  
297 tions contributing to decoding success. During the 0-500 ms  
298 window, item-level decoding was driven by occipital activity,  
299 resembling the EEG distributions found in the Perceptual  
300 Baseline condition during the same window (Figure 4F, 4H).  
301 Strikingly, during the 500-3000 ms, there were no brain regions  
302 that contributed significantly to item-level decoding (Figure  
303 4G), suggesting that suppression had abolished evidence for  
304 cortical reinstatement of scene memories.

305 In addition to scalp EEG distributions revealed by the  
306 channel searchlight analysis, confusion matrices of item-level  
307 decoding provided converging evidence supporting the hypoth-

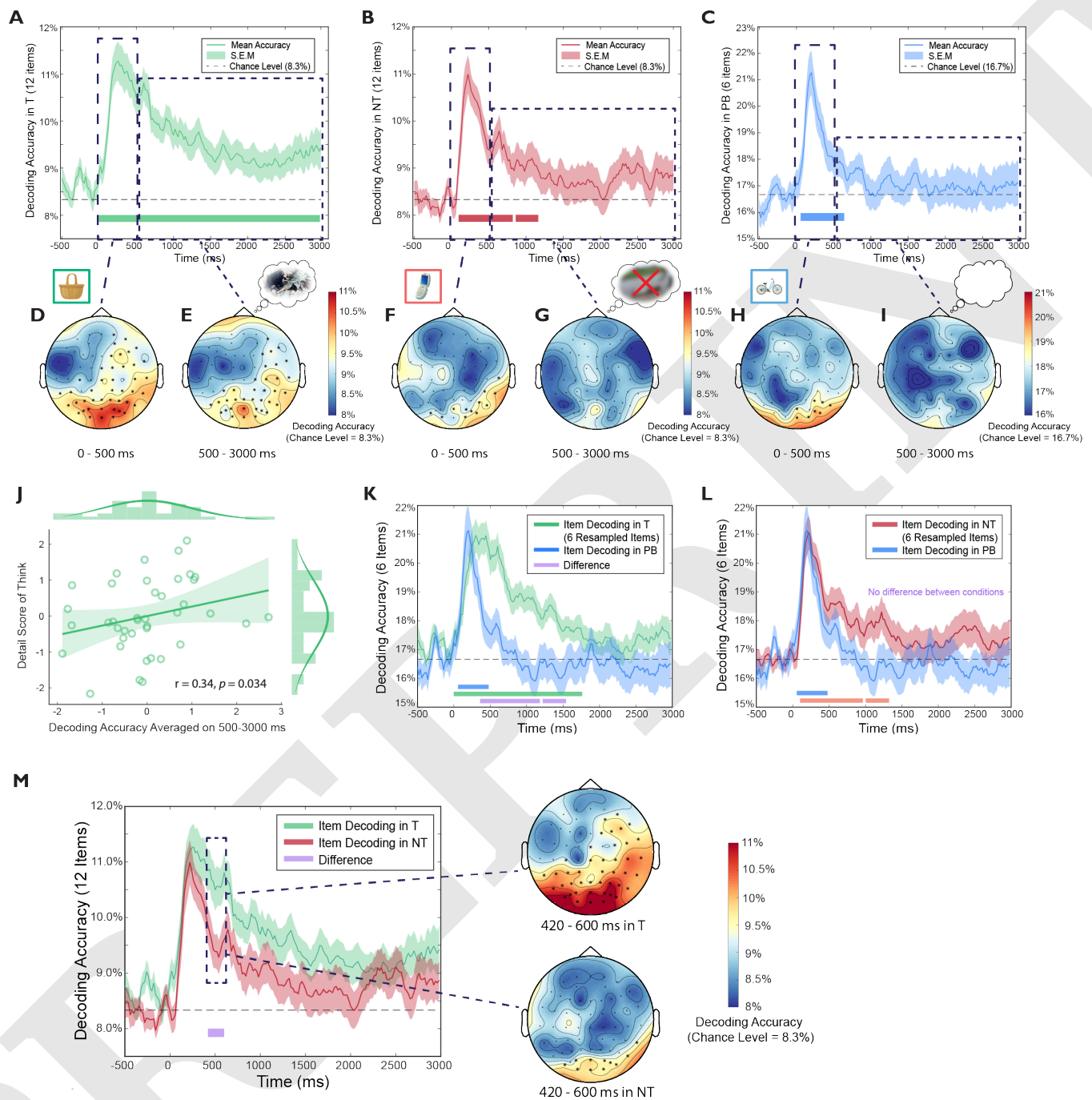


**Fig. 4.** Item-level Time Domain Decoding. (A-C) The item-level decoding patterns (averaged across participants) in each retrieval condition. Lines at the bottom indicate significant time clusters against chance level, with permutation cluster correction ( $\alpha_s = 0.05$ ). (D-I) Channel searchlight analyses of time domain decoding during an early (0-500 ms) and a later time window (500-3000 ms). The colorbar indicates decoding accuracy. Electrodes with significant decoding accuracies are highlighted (permutation cluster corrected,  $\alpha_s = 0.05$ ). (J) During Think trials, decoding accuracies averaged on 500-3000 ms predicted the number of details recalled from emotional scenes. (K) Item-level decoding in the Think condition (using 6 resampled items) is higher than it is in the Perceptual Baseline condition from 360-1180 ms,  $p_{corrected} < .001$  and from 1220-1540 ms,  $p_{corrected} = .022$ . Lines at the bottom indicate cluster-corrected significant time clusters against the chance level (green and blue for Think and Perceptual Baseline) or the difference between the two conditions (purple). (L) Item-level decoding in the No-Think condition (using 6 resampled items) is not significantly different from decoding in the Perceptual Baseline condition. Lines at the bottom indicate significant time clusters against the chance level (red and blue for No-Think and Perceptual Baseline conditions, respectively). (M) Retrieval suppression significantly reduced item-level decoding accuracies from 420-600 ms compared to retrieval (Think condition), with the right panel showing channel searchlight analyses on this time window.

308 sized stages of retrieval suppression: we observed significant  
309 above-chance item-specific classifications in all three condi-  
310 tions during the first 500 ms, when cue-processing might be  
311 expected to predominate; in contrast, distinctive classification  
312 patterns remained only in the Think condition during 500-  
313 3000 ms (Figure S3C-E). Thus, suppression reduced cortical  
314 patterns during No-Think trials to the extent that they were  
315 as uninformative as items in our perceptual baseline condition,  
316 in which no scene retrieval was possible.

317 To precisely characterize of the temporal dynamics of re-  
318 trieval suppression, we contrasted the time-dependent evolu-  
319 tion of item-specific cortical patterns between retrieval suppres-  
320 sion and both the retrieval and perceptual baseline conditions.  
321 A direct comparison of Think vs. No-Think item-level de-  
322 coding revealed that retrieval suppression reduced decoding  
323 accuracies from 420 to 600 ms ( $p_{\text{corrected}} = .044$ , Figure 4M  
324 left panel). Searchlight analyses during 420-600 ms revealed  
325 that, whereas voluntary retrieval engaged item-specific brain  
326 activity over frontal-parietal-occipital regions, retrieval sup-  
327 pression was only associated with occipital activity (Figure  
328 4M right panel). When No-Think trials were directly com-  
329 pared to Perceptual Baseline trials (using 6 randomly sampled  
330 items from the No-Think condition), there were no significant  
331 decoding accuracy differences during the entire 0-3000 epoch  
332 (none of the differences survived permutation correction, see  
333 Figure 4L).

334 Reduced decoding accuracy for individual No-Think items  
335 in the 420-600ms window suggests that the retrieval stopping  
336 process may begin to exert its first effects within this window,  
337 a possibility consistent with findings from our condition-level  
338 decoding analyses. We next sought to determine whether  
339 prefrontal-control processes were linked to suppressed item-  
340 level decoding. Consistent with this possibility, we found  
341 that in the No-Think (vs. Think) trials, reduced item-level  
342 decoding was preceded by enhanced 200-400 ms theta power  
343 over midline and right prefrontal cortex (Figure 3I). Critically,  
344 theta power elevation across this region positively correlated  
345 with the 420-600 ms decoding accuracy reduction ( $r = 0.30$ ,  
346  $p = .064$ , Figure S3F), suggesting that processes indexed by  
347 higher theta power (No-Think > Think) contributed to lower  
348 item-specific decoding accuracies (No-Think < Think).

349 Together with the evidence for suppression-specific patterns  
350 in the condition level analysis, these item-level decoding results  
351 reveal a precise timeline of how retrieval suppression unfolded:  
352 inhibitory control was engaged within the first 500 ms upon  
353 encountering a unwelcome reminder cue, presumably before  
354 the cue-to-memory conversion process completed, to obstruct  
355 retrieval and prevent reinstatement from happening. This early  
356 control weakened, and eventually abolished memory-specific  
357 cortical patterns during 500-3000 ms.

358 **Rapid and Sustained Suppression of Individual Memories**  
359 **Led to Their Forgetting.** To understand how the temporal dy-  
360 namics of retrieval suppression influenced later forgetting of  
361 suppressed content, we divided participants into *High-* vs. *Low-*  
362 *Suppression Groups* based on a median-split of suppression-  
363 induced forgetting scores. We focused on below-baseline for-  
364 getting (i.e., NT-minus-BL *Detail* scores) using our detail  
365 measure of scene recall. We tested the hypothesis that suc-  
366 cessful suppression-induced forgetting was associated with a  
367 greater reduction in decoding accuracy during No-Think trials  
368 compared to Think trials, compared to unsuccessful forget-

369 ting. In the High-Suppression group (Figure 5A), suppression  
370 significantly reduced item-specific decoding accuracy during  
371 No-Think (vs. Think) trials during two time windows: 300-680  
372 ms ( $p_{\text{corrected}} = .006$ ) and 1140-1400 ms ( $p_{\text{corrected}} = .031$ ).  
373 By contrast, in the Low-Suppression group (Figure 5B), the  
374 same comparison revealed no NT vs. T decoding accuracy  
375 differences, indicating that evidence for item-specific decoding  
376 remained possible for this group, despite their efforts to sup-  
377 press. In the high forgetting group, the observed differences  
378 may reflect an early disruption of cue-to-memory conversion  
379 processes occurring at around 500 ms, and a later weakening  
380 of item-specific cortical reinstatement between 1000-1500 ms.  
381 Corroborating a role of early and timely suppression in forget-  
382 ting, item-level decoding accuracy during the early 300-680 ms  
383 window predicted later suppression-induced forgetting across  
384 all participants ( $r = 0.35$ ,  $p = .027$ , Figure 5C). Thus, the  
385 more effectively participants suppressed unwanted memories  
386 during the 300-680 ms window, the more successful was the  
387 later forgetting of scene details.

388 We next compared item-level decoding accuracy between  
389 the No-Think (using 6 randomly sampled items) and Per-  
390 ceptual Baseline conditions in the Low and High-Suppressor  
391 groups. Strikingly, we found no between-condition differences  
392 in the *High-Suppression Group* (Figure 5D), indicating that  
393 suppression reduced pattern information so effectively that  
394 the brain activity contained no evident item-specific content,  
395 mimicking those trials in which there was actually no scene to  
396 reinstate. In contrast, participants from the *Low-Suppression*  
397 *Group* showed significantly higher decoding accuracies during  
398 No-Think trials compared to Perceptual Baseline trials, pri-  
399 marily toward the end of the suppression epoch (i.e., 2300-2560  
400 ms,  $p_{\text{corrected}} = .029$ , Figure 5E, purple dashed outline). Thus,  
401 less successful forgetting was associated with relapses in the  
402 activation of suppressed content during sustained control of  
403 unwanted memories. Together, these results highlight that not  
404 only early and rapid, but also sustained control are important  
405 in successful suppression-induced forgetting.

406 **Theta and Alpha Oscillations Track Item-Level Perception and**  
407 **Reinstatement Processes, Respectively.** We sought converging  
408 evidence for the active suppression of individual memories  
409 by tracking item-specific oscillatory activity in the theta and  
410 alpha bands. Theta and alpha activity have been implicated in  
411 perceptual and memory-related processes, such that theta may  
412 reflect sensory intake and hippocampo-cortical communication  
413 loops (Bastos et al., 2015; Colgin, 2013), and alpha may  
414 track neocortex-dependent memory reinstatement processes  
415 (Staresina et al., 2019; Staresina & Wimber, 2019). If so,  
416 posterior theta activity may enable item-specific decoding of  
417 the cue objects themselves, whereas alpha activity may enable  
418 decoding of reinstated scenes.

419 In all three conditions, we found that theta activity in the 0-  
420 500ms window over occipital regions significantly distinguished  
421 among individual items, consistent with theta's putative role  
422 in visual processing of individual cue objects ( $p_{\text{Scorrected}} < .001$ ,  
423 Figure 6A-C, also see Figure 6D-G). During the 500-3000 ms  
424 window in which scene recollection could unfold, both theta  
425 and alpha power drove significant decoding accuracy during  
426 Think trials (theta:  $p_{\text{Scorrected}} < .027$ ; alpha:  $p_{\text{Scorrected}} < .039$ ,  
427 Figure 6D). Critically, however, retrieval suppression during  
428 No-Think trials abolished any evidence for item-specific decod-  
429 ing based on theta or alpha band activity (Figure 6E). There

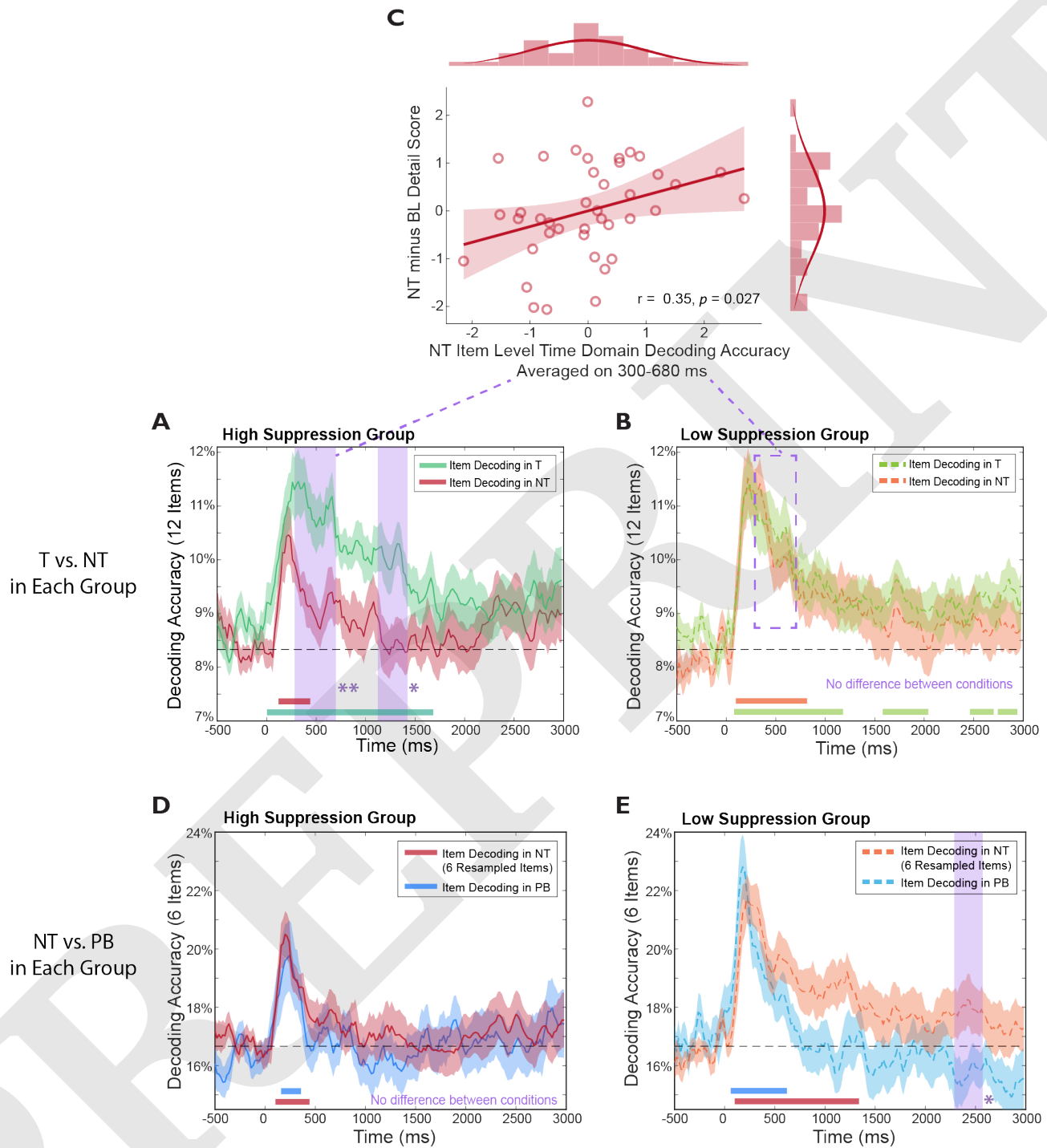


**Fig. 5.** Item-level Decoding Results in High- and Low-Suppression Groups. (A, B) Comparisons between Think and No-Think item-level decoding in High-/Low-Suppression Groups, respectively. In the High-Suppression Group, the Think vs. No-Think difference was significant during the 300-680 ms and 1140-1400 ms windows, whereas no differences were found in the Low-Suppression Group. (C) Across both groups, the averaged decoding accuracy during the 300-680 ms. window positively correlated with participant's suppression-induced forgetting (i.e. No-Think - Baseline of the detail index). (D, E) Resampled item-level decoding comparisons between the No-Think and Perceptual Baseline conditions in the High- and Low-Suppression Groups, respectively. In the High-Suppression Group, the No-Think condition did not differ from the Perceptual Baseline condition in item-level decoding accuracy, despite both showing above chance decoding within the 0-500 ms window. In the Low-Suppression Group, in contrast, a significant difference between the No-Think and the Perceptual Baseline conditions was observed during the 2300-2560 ms window. Colored bars at the bottom of each figure denote time clusters that were significantly above chance (permutation corrected, one-sided  $\alpha s = 0.05$ ). Purple dashed outlines denote significant time clusters between conditions/groups (permutation corrected, two-sided  $\alpha s = 0.05$ ).

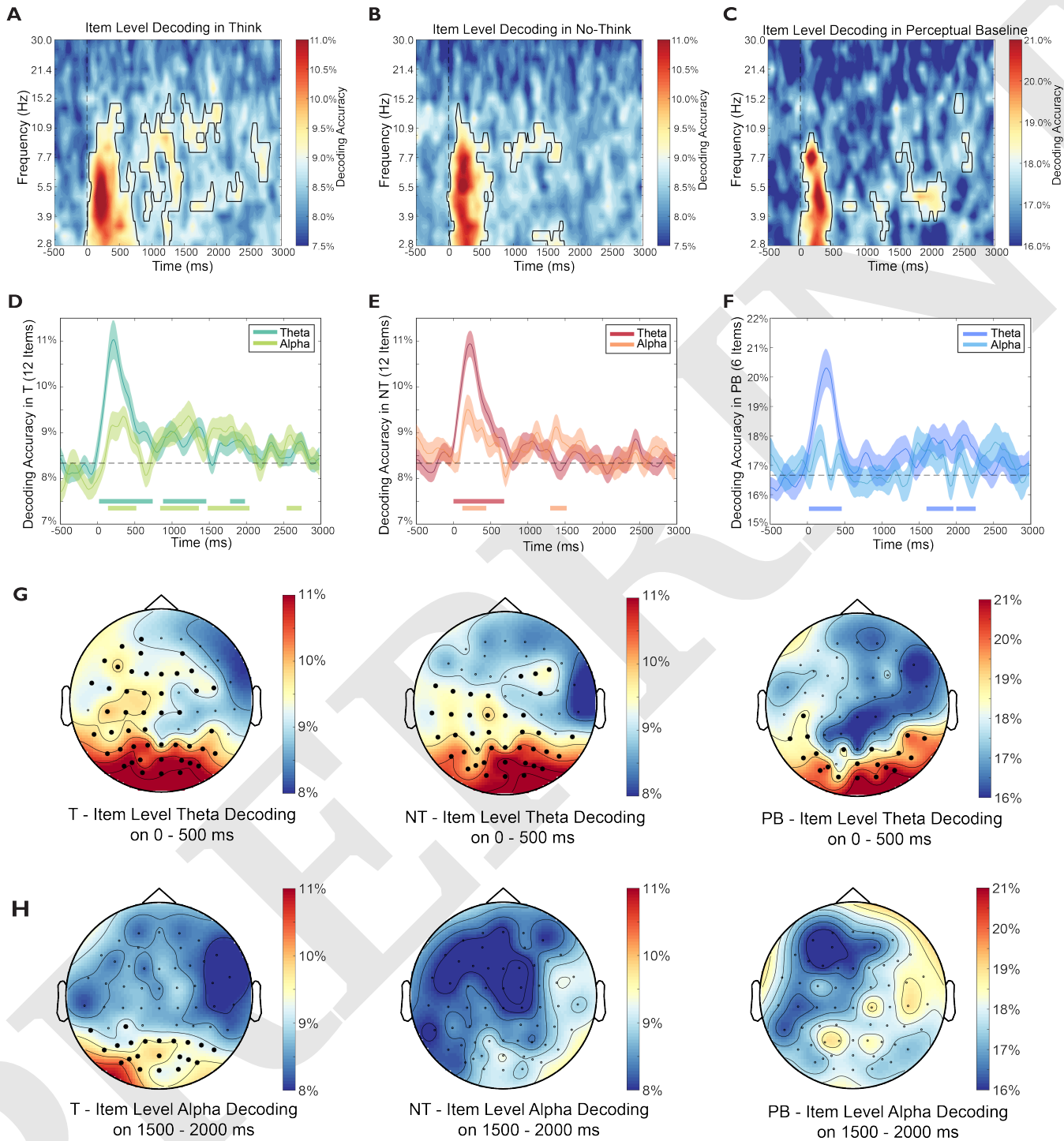


**Fig. 6.** Item-level Time-Frequency Domain Decoding. (A-C) Item-level time-frequency decoding results. Frequency is log scaled and the colorbar denotes decoding accuracy. The black outline highlights significant clusters against chance levels (both cluster  $\alpha$  and permutation  $\alpha$  are 0.05, one-sided). (D-F) Decoding accuracies in A-C are averaged on theta and alpha bands. Horizontal bars denote significant clusters of the band-averaged accuracies against chance level (cluster corrected, one-sided  $\alpha_s = 0.05$ ). (G) Item-level theta searchlight during the 0-500 ms window showed an occipital distribution in all three conditions. Significant channels are highlighted (permutation cluster corrected with one-sided  $\alpha_s = 0.05$ ). (H) Item-level alpha searchlight during the 1500-2000 ms window showed that only in the Think condition was alpha power able to distinguish among items. The alpha searchlight decoding in the Think condition originated from the posterior region. Significant channels are highlighted (permutation cluster corrected with one-sided  $\alpha_s = 0.05$ ).

430 was short-lived theta-driven decoding in Perceptual Baseline  
431 trials, which may reflect occasional perceptual processing of  
432 objects (theta:  $p_{\text{corrected}} < .011$ , Figure 6F). Channel search-  
433 light analyses during the 500-3000 ms window revealed that  
434 alpha activity over the occipital-parietal region contributed  
435 to decoding performance in the Think condition, but did not  
436 in either the No-Think or Perceptual Baseline conditions (see  
437 Figure 6H). These findings support the possibility that alpha  
438 activity is linked with scene-specific memory reinstatement  
439 processes and not simply to object perception. If so, the lack  
440 of significant alpha-based decoding in No-Think trials reflects  
441 the abolition of memory reinstatement processes arising due  
442 to active suppression.

## 443 Discussion

444 Suppressing memory retrieval requires effort; it is not simply  
445 neglecting to engage retrieval when an unwelcome reminder  
446 appears, but instead involves an active inhibition process (An-  
447 derson & Hulbert, 2020; Wimber et al., 2015). Applying  
448 multivariate pattern analyses during the think/no-think task,  
449 we observed, for the first time, how individual aversive memo-  
450 ries are suppressed in real time. Our precise chronometry of  
451 retrieval suppression provides new knowledge about the time  
452 windows and neural activity critical to achieving successful for-  
453 getting. We found that effective forgetting is associated with 1)  
454 the rapid deployment of inhibitory control in suppressing cor-  
455 tical patterns within the first 500 ms, supported by enhanced  
456 midfrontal theta activity during efforts to stop retrieval; and  
457 2) sustained control applied to abolish item-specific cortical  
458 EEG patterns reflected in the spatial pattern of theta and  
459 alpha activity during the 500-3000 ms window.

460 Three findings suggest that an early, active control process  
461 truncates retrieval of highly specific, individual memories, in-  
462 ducing later forgetting. First, when a reminder cue appeared,  
463 within 500 ms retrieval suppression enhanced midfrontal and  
464 right prefrontal theta activity relative to active retrieval and  
465 also relative to a perceptual baseline condition in which scene  
466 retrieval was impossible. Given evidence linking frontal mid-  
467 line theta and inhibitory control (Cavanagh & Frank, 2014;  
468 Crespo-García et al., 2021; Nigbur et al., 2011), this find-  
469 ing is consistent with the possibility that attempts to stop  
470 the retrieval process engaged inhibitory control. This finding  
471 suggests a rapid onset of inhibitory control in the face of an  
472 unwelcome reminder, but does not, by itself, link that control  
473 process to the successful exclusion of unwanted memories from  
474 awareness.

475 Second, whereas we detected significant item-specific brain  
476 activity during active retrieval, retrieval suppression reduced  
477 the ability to detect individual items during the 420-600 ms  
478 time window. The ability to detect reduced item-specific ac-  
479 tivity in such an early time window indicates that suppression  
480 rapidly interrupts the retrieval process. Estimates based on in-  
481 tracranial recordings suggest that beginning at around 500 ms,  
482 hippocampus-dependent pattern completion would normally  
483 trigger cortical reinstatement of target memories, accompanied  
484 by vivid recollection (Colgin, 2016; Lavenex & Amaral, 2000;  
485 Staresina & Wimber, 2019). Given this timing, successful  
486 retrieval suppression ideally should target prior to this time  
487 window to pre-empt or truncate the cue-to-memory conversion  
488 processes, preventing memories from being reinstated. Indeed,  
489 our putative index of inhibitory control predicted reduced item-

490 specific EEG activity: we found that elevated theta power in  
491 the 200-400 ms window predicted later reductions of item-level  
492 decoding accuracy in the 420-600ms window. These findings  
493 suggest that enhanced inhibitory control disrupted the cue-to-  
494 memory conversion process to prevent aversive memories from  
495 being retrieved, but it does not link such changes in cortical  
496 reinstatement to later forgetting of the suppressed content.

497 Third, we found that reduced item-specific cortical pat-  
498 tern information during this early time window predicted later  
499 suppression-induced forgetting. Specifically, whereas those par-  
500 ticipants showing high suppression-induced forgetting exhib-  
501 ited significantly reduced item-level decoding accuracies during  
502 suppression, compared to retrieval in the 300-680 ms win-  
503 dow, Low-Suppression participants did not. In general, across  
504 all participants, reduced No-Think item decoding accuracies  
505 within the 300-680 ms window predicted later suppression-  
506 induced forgetting. These results link the early engagement  
507 of control not only to reduced reinstatement, but also to an  
508 increased capacity to forget the suppressed content. Given  
509 that hippocampus-dependent pattern completion processes  
510 emerge at around 500 ms (Staresina & Wimber, 2019), this  
511 finding again suggests that for successful forgetting to occur,  
512 top-down inhibitory control should be engaged quickly be-  
513 fore and during the cue-to-memory conversion time window,  
514 preventing cortical reinstatement.

515 The temporal evolution of item-specific cortical patterns  
516 suggests that whereas rapid control is important to successful  
517 forgetting, sustained control also is necessary. Whereas re-  
518 trieval suppression weakened the ability to detect item-specific  
519 cortical patterns starting from ~400 ms after cue-onset, indi-  
520 vidual memories could still be identified until 1200 ms post-cue.  
521 Residual item-specific cortical patterns during the 420-1200  
522 ms window clearly call for sustained control to ensure that  
523 unwanted memories are suppressed. The ability to detect item-  
524 specific cortical patterns was fully abolished by 1200 ms for  
525 the remainder of the 3000ms trial. The maintenance of control  
526 over this longer time period appears to be reflected in reduced  
527 alpha power throughout the trial. Together, these temporal  
528 characteristics reveal a timeline for the suppression of aversive  
529 scenes: early control processes truncate retrieval during the  
530 perception-to-memory conversion time window (e.g., ~420-  
531 600 ms), with sustained control processes down-regulating  
532 unwanted memories (e.g., ~1200 ms), eventually abolishing  
533 item-specific cortical patterns (1200-3000 ms).

534 Two additional findings underscore the importance for sus-  
535 tained control in the successful forgetting of unwanted mem-  
536 ories. Although early control clearly was instrumental to  
537 successful forgetting, we also found evidence that activity in  
538 later time windows was also functionally relevant. First, those  
539 participants showing higher suppression-induced forgetting  
540 showed significantly reduced item-level decoding accuracies  
541 during suppression than during retrieval in the 1140-1400 ms  
542 time window, suggesting the functional importance of sus-  
543 tained control. Second, low-suppression participants showed  
544 evidence of an ironic rebound effect later in the trial: retrieval  
545 suppression was associated with significantly higher decoding  
546 accuracies than our perceptual baseline trials in the 2600-2800  
547 ms time window. This apparent rebound effect in cortical  
548 reinstatement suggests that participants who later showed less  
549 successful forgetting suffered relapses in controlling unwanted  
550 memories, particularly towards the end of retrieval suppres-

551 sion (van Schie & Anderson, 2017). Taken together, these two  
552 findings illustrate that successful forgetting requires sustained  
553 suppression of individual memories during the prolonged cortical  
554 reinstatement time window.

555 Our item-level decoding results during voluntary retrieval  
556 trials (i.e., Think trials) provide converging evidence for our  
557 staged view of how cued memory recall unfolds. To determine  
558 whether sustained item-level decoding during Think trials  
559 might simply reflect persisting attention to individual object  
560 cues, we showed that 1) the early (0-500 ms) vs. late (500-3000  
561 ms) decoding patterns were characterized by distinct EEG  
562 spatial distributions, and 2) only the 500-3000 ms item-level  
563 decoding accuracy predicted more detail of scene recall of  
564 Think items on the later test. These results suggest that  
565 whereas the early decoding pattern reflects perceptual processes  
566 acting on item-specific cues, the later decoding pattern  
567 likely reflects the successful recollection of the accompanying  
568 scene. Consistent with this interpretation, both theta and  
569 alpha power contributed to item-level decoding during voluntary  
570 retrieval, with an early onset of occipital theta activity  
571 followed by parietal-occipital alpha activity. Theta and alpha  
572 activities have been implicated in perceptual and memory-  
573 related processes, such that theta may reflect sensory intake  
574 and hippocampo-cortical communication loops (Bastos et al.,  
575 2015; Colgin, 2013). Relatedly, linking behavioral oscillation  
576 and neural oscillation, a recent study demonstrated a prominent  
577 role of theta rhythm in memory retrieval (Ter Wal et al., 2021).  
578 Regarding alpha, previous research suggests that alpha may track  
579 neocortex-dependent memory reinstatement processes (Staresina et al., 2019;  
580 Staresina & Wimber, 2019). Decoding patterns during Perceptual  
581 Baseline trials provided converging support for this account: when  
582 participants viewed object cues that lacked any associated scene  
583 memory, only occipital theta activity in the 0-500ms window  
584 drove significant item-level decoding, ruling out any contribution  
585 of scene retrieval.

587 If the foregoing staged view of retrieval is correct, then  
588 item-specific decoding based on alpha-band activity after initial  
589 cue processing may reflect the reinstatement of individual  
590 scenes. Indeed, previous research has found that memory  
591 reinstatements are associated with alpha oscillations. For example,  
592 in a directed forgetting task, Fellner et al. (2020) reported  
593 alpha power increases 1000-2000 ms following to-be-remembered  
594 cues, which were associated with selective rehearsal (see also  
595 Bäuml et al., 2008; Hanslmayr et al., 2012; Xie et al., 2020).  
596 Mirroring this, we found that voluntary retrieval enhanced  
597 alpha power during the same 1000-2000 ms window when  
598 reinstatement of the associated scene would be expected (Figure  
599 S1H-M). If this interpretation is correct, then the reduced  
600 alpha power relative to our perceptual baseline condition (and  
601 alpha-based item-level decoding performance), likely reflects  
602 the outcome of suppressing scene reinstatement. Critically,  
603 higher decoding based on alpha activity during retrieval  
604 suppression, relative to the perceptual baseline condition  
605 predicted later suppression-induced forgetting. Suppression-  
606 induced alpha power reductions may reflect reduced memory  
607 reinstatement (Hanslmayr et al., 2012; Waldhauser et al., 2015),  
608 which contributed to episodic forgetting.

609 Taken together, our findings show that for successful  
610 retrieval suppression and forgetting, inhibitory control needs to  
611 be both fast and sustained. On the one hand, early enhanced

612 frontal theta disrupted cue-to-memory conversion, truncat-  
613 ing the reinstatement of individual aversive scene memories  
614 within the first 500 ms upon seeing the cues. On the other  
615 hand, sustained control weakened and eventually abolished  
616 item-specific cortical EEG patterns during the 500-3000 ms  
617 time window, reflected in reduced alpha activity. In contrast,  
618 both diminished early control and relapses during later  
619 sustained control compromised successful voluntary forgetting of  
620 suppressed content. By tracking the precise timing and neural  
621 dynamics of retrieval suppression in modulating individual  
622 memories, our results may inform future research on when  
623 and how to intervene during retrieval suppression to improve  
624 people's ability to forget unwanted memories.

## 625 Materials and Methods

626 **Experimental Subject Details.** Forty-one participants (mean  
627 age = 19.57, age range: 18-23 years, 26 females) were recruited  
628 from the University of Hong Kong. One participant was  
629 excluded due to non-compliance of task instructions (details  
630 see Materials and Procedure). Ethical approval was obtained  
631 from the Human Research Ethics Committee of The University  
632 of Hong Kong.

633 **Materials and Procedure.** We used 42 object-scene picture  
634 pairs from Küpper et al. (2014). Scenes depict aversive  
635 contents such as natural disasters, assault, injury, etc. Each  
636 object resembled an item from its paired negative scene, thus  
637 establishing naturalistic and strong associations. Six pairs were  
638 used for instruction and practice purposes. The remaining  
639 36 pairs were equally divided into 3 sets, with 12 pairs in  
640 each of three following conditions: Think, No-Think, and  
641 Baseline. Picture pairs used in the three conditions were  
642 matched on valence and arousal, and were counterbalanced  
643 across participants. Another 6 objects without any paired  
644 scenes were used as Perceptual Baseline trials, which did  
645 not involve any memory retrieval. Participants completed  
646 the following sessions in order: Encoding, Think/No-think  
647 (TNT) and Cued Recall. At the end of the study, participants  
648 completed a 3-item, instruction compliance questionnaire.

649 **Encoding.** Participants were presented with 42 object-scene  
650 pairings, plus 6 objects from Perceptual Baseline. Each object-  
651 scene pair was presented on an LCD monitor for 6 s with an  
652 inter-trial-interval (ITI) of 1s. Participants were instructed  
653 to pay attention to all the details of each scene, and to  
654 associate the left-sided object and the right-sided scene. They  
655 next completed a test-feedback session, in which each object was  
656 presented up to 4 s until participants pressed a button indicating  
657 whether they could recall the associated scene or not. If  
658 participants gave a 'yes' response, they were presented with  
659 three scenes from the learning phase and needed to identify the  
660 correct one within another 4 s. Regardless of accuracy, the  
661 correct pairing would be presented for 2.5 s. This test-feedback  
662 cycle repeated until participants reached 60% accuracy. Twenty-  
663 six participants reached this criterion in the first cycle, 13  
664 participants in two, and 1 in three. Following the test-feedback  
665 cycles, participants completed a recognition-without-feedback  
666 test, so as to confirm that items from different conditions were  
667 encoded at comparable levels before the TNT session ( $ps >$   
668 .104).

669 **TNT.** Participants were presented with 24 objects from the 36  
670 object-scene pairings, with 12 objects in each of the Think or  
671 No-think conditions, respectively. The remaining 12 objects  
672 were not shown in the TNT and were used in the Baseline  
673 condition. These 24 objects were presented in either yellow- or  
674 blue-colored frames indicating think and no-think conditions,  
675 with colors counterbalanced across participants. Six objects  
676 (without any pairing scenes) were presented in white-colored  
677 frames and served as Perceptual Baseline trials. Thus, 30  
678 unique objects were shown in the TNT session. Each object  
679 was presented 10 times, resulting in a total of 300 trials. Each  
680 trial began with a fixation cross (2-3s), followed by the object  
681 in a colored frame for 3s. The ITI was 1 s.

682 For Think trials, participants were instructed to try their  
683 best to think about the objects' associated scenes in detail,  
684 and to keep the scenes in mind while the objects remained  
685 on the monitor. For No-Think trials, participants were given  
686 direct-suppression instructions: they were told to pay full  
687 attention to the objects while refraining from thinking about  
688 anything. If any thoughts or memories other than the objects  
689 came to mind, they needed to try their best to push the  
690 intruding thoughts/memories out of their mind and re-focus  
691 on the objects. Participants were also prohibited from using  
692 any thought substitution strategies (i.e., thinking about a  
693 different scene). For Perceptual Baseline trials, participants  
694 were simply instructed to focus on the object.

695 **Cued Recall.** Following the TNT session, participants were pre-  
696 sented with each of the 36 objects from Think, No-Think and  
697 Baseline conditions. Each object was presented at the center  
698 of the monitor, alongside a beep sound prompting participants  
699 to verbally describe the associated scenes within 15 s. The  
700 ITI was 3 s. Participants' verbal descriptions were recorded  
701 for later scoring. Perceptual Baseline objects were not shown  
702 in this recall test because they were not paired up with any  
703 scenes.

704 **Cued Recall Analyses.** Two trained raters who were blind to  
705 experimental conditions coded each of the verbal descriptions  
706 along three dimensions following the criteria used in in a  
707 previous study (Küpper et al., 2014), namely *Identification*,  
708 *Gist* and *Detail*. Each measure focused on different aspects  
709 of memories: Identification referred to whether the verbal  
710 description was clear enough to correctly identify the unique  
711 scene, and was scored as 1 or 0. Inconsistent ratings were  
712 resolved by averaging 0 and 1, resulting in a score of 0.5. Gist  
713 measured whether participants' verbal descriptions contained  
714 critical elements pertaining to the scene's main themes. Two  
715 independent raters identified two to four gists for each scene  
716 (Küpper et al., 2014). We scored gist as proportion, using  
717 the number of correct gists from participants' verbal report  
718 divided by all possible gists for each scene. Detail measured  
719 how many correct meaningful segments were provided during  
720 the verbal description, and was scored on the number of details.  
721 Interrater agreement for the scoring of all three measures was  
722 high: Identification  $r = 0.71$ , Gist  $r = 0.90$ , Detail  $r = 0.86$ .

723 **EEG Recording and Preprocessing.** Continuous EEGs were  
724 recorded during the TNT session using ANT Neuro eego  
725 with a 500 Hz sampling rate (ANT, The Netherlands), from  
726 64-channel ANT Neuro Waveguard caps with electrodes posi-  
727 tioned according to the 10-5 system. The AFz served as the  
728 ground and CPz was used as the online reference. Electrode

impedances were kept below 20 kilo-ohms before recording. Eye movements were monitored through EOG channels.

Raw EEG data were preprocessed in MATLAB using EEGlab Toolbox (Delorme & Makeig, 2004) and ERPlab Toolbox (Lopez-Calderon & Luck, 2014): data were first down-sampled to 250 Hz, and were band-passed from 0.1 to 60 Hz, followed by a notch filter of 50Hz to remove line noise. Bad channels were identified via visual inspection, and were removed and interpolated before re-referencing to common averages. Continuous EEG data were segmented into -1000 to 3500 ms epochs relative to the cue onset, and baseline corrected using -500 to 0 ms as baseline period. Next, independent component analyses (ICAs) were implemented to remove eye blinks and muscle artifacts. Epochs with remaining artifacts (exceeding  $\pm 100 \mu\text{V}$ ) were rejected. The numbers of accepted epochs used in all following analyses were comparable across Think (Mean  $\pm$  SD,  $100.33 \pm 11.57$ ) and No-think ( $103.18 \pm 10.61$ ) conditions. Valid trials number in Perceptual Baseline is  $56.58 \pm 3.23$ . All EEG analyses were based on 61 electrodes, excluding EOG, M1, M2, AFz (ground) and CPz (online reference).

**Condition-/Item-level Decoding with Time Domain EEG.** Decoding analyses were conducted in MATLAB using scripts adapted from (Bae & Luck, 2018), which used a support vector machine (SVM) and error-correcting output codes (ECOC). The ECOC model combined results from several binary classifiers for prediction output in multiclass classification.

In condition-level decoding, we used one-vs-one SVMs to perform pairwise decoding among the three conditions (Think vs. Perceptual Baseline, No-Think vs. Perceptual Baseline, and Think vs. No-Think). For Think vs. Perceptual Baseline and No-Think vs. Perceptual Baseline condition-level decoding, we first subsampled trials in T/NT to be comparable with Perceptual Baseline so that each condition had about 56 trials. We next divided EEG trials from each condition into 3 equal sets and averaged EEG epochs within each set into sub-ERPs to improve signal-to-noise ratio. The decoding was achieved within each participant from -500 to 3000 ms using these sub-ERPs in a 3-fold cross validation: each time 2 of the 3 sub-ERPs are used as training dataset with the condition labels, and the remaining one was used as testing dataset. After splitting training and testing datasets, sub-ERPs were both normalized using the mean and standard deviation of training dataset to remove ERP-related activity. This process was conducted on every 20 ms time point (subsampled to 50 Hz), and repeated for 10 iterations. We were comparing condition-level decoding accuracy against its chance level, 50%, given two conditions were involved in each pairwise decoding.

For item-level decoding, we used one-vs-all SVMs to decode each individual stimulus within each condition, separately. Decoding procedures were the same as condition-level decoding. Thus, the trial numbers of each stimulus are first matched to the least one within each participant (at most 10 trials, if no trial was rejected). Then, all trials of each stimulus were divided into 3 sets before averaging and the 3-fold cross validation. Both training dataset and testing dataset were normalized using the mean and standard deviation of training dataset. The decoding process was conducted on every 20 ms time point and for 10 iterations (results remained the same for up to 100 iterations, see supplementary Figure S3G). For Think and No-Think conditions, the chance levels were 1/12

790 (8.33%) given that there were 12 unique stimuli in each of these  
791 two conditions. For Perceptual Baseline trials, the chance level  
792 was 1/6 (16.67%).

793 Given we had different item numbers in Perceptual Baseline  
794 (6 items) and Think/No-Think (12 items), in order to directly  
795 compare the decoding accuracy in Think or No-Think with  
796 Perceptual Baseline, we conducted a resampled decoding in  
797 Think and No-Think, respectively. The resampled decoding  
798 is similar to the normal decoding, except that during each  
799 iteration we randomly selected 6 out of all 12 items before  
800 dividing and averaging into 3 sets. Considering the random-  
801 ization used only half of the items, we increased iterations  
802 to 20 times. An item-level decoding with 20-iterations was  
803 also rerun in Perceptual Baseline, to be compared with the  
804 resampled decoding.

#### 805 **Condition-/Item-level Decoding with Time-Frequency Domain EEG.**

806 Time domain EEG was wavelet transformed into time-  
807 frequency domain data in Fieldtrip Toolbox (Oostenveld et al.,  
808 2011) before decoding. Frequencies of interest increased loga-  
809 rithmically from 2.8 Hz to 30 Hz, resulting in 22 frequency bins.  
810 Wavelet cycles increased linearly along with frequencies from  
811 3 to 7. Then the decoding was conducted for each frequency  
812 bin data across time in the same procedure as described in  
813 Condition-/Item-level Decoding with Time Domain EEG (as  
814 if treating each frequency bin data as a time domain data).

815 **Channel Searchlight Decoding.** Both condition- and item-level  
816 decoding used EEGs from all 61 channels as features. To  
817 examine which electrodes contributed the most to the decoding  
818 accuracy, we conducted a channel searchlight decoding using  
819 subsets of the 61 channels as features (Treder, 2020).

820 Specifically, we first divided all channels into 61 neigh-  
821 bourhoods, centering each channel according to its location  
822 (conducted in Fieldtrip Toolbox (Oostenveld et al., 2011)  
823 via `ft_prepare_neighbours()` function using ‘triangulation’  
824 method). Immediately neighbouring channels were clustered  
825 together, resulting in  $6.39 \pm 1.50$  channel neighbours for each  
826 channel (with overlaps). Then the time domain EEG was  
827 averaged on time windows of interest, i.e., averaged on 0-500  
828 ms, 500-3,000 ms, etc., to inspect the decoding topographical  
829 distribution on different time windows. The rest of the pro-  
830 cedure was the same as time domain EEG decoding: we divided  
831 data into 3 sets and averaged within each set before splitting  
832 training and testing datasets; then we normalized them using  
833 mean and standard deviation of training sets. Finally, the  
834 decoding was conducted with a 3-fold cross validation and  
835 10 iterations. Theta/alpha searchlight was conducted in the  
836 same way as time-domain searchlight, after averaging time-  
837 frequency power on respective oscillation range (theta: 4-8 Hz;  
838 alpha: 9-12 Hz).

839 **Time Frequency Analyses.** Six electrode clusters were selected for  
840 Time Frequency analyses: left parietal (CP3/5, P3/5), parietal  
841 (Pz, CP1/2, P1/2), right parietal (CP2/4, P2/4), frontocentral  
842 (FC1/2, C1/2, FCz, Cz), left prefrontal (AF3, F3/5) and right  
843 prefrontal (AF4, F4/6).

844 Time frequency transformation was performed using the  
845 same parameters as in decoding analyses in Fieldtrip (Oost-  
846 enveld et al., 2011), with additional decibel baseline normal-  
847 ization using power on -500 to -200 ms. We focus on the  
848 early theta power change on 200-400 ms which is indicator  
849 of inhibitory control (Cavanagh & Frank, 2014; Nigbur et al.,

2011), and theta and alpha power change on a post hoc late  
time window (500-3000 ms) following condition level decoding  
results.

**Correlation Analyses.** We calculated Spearman’s Rho for all cor-  
relations. In condition-level decoding, memory of Think and  
No-think was normalized by subtracting and then divided by  
Baseline memory, then correlated with time domain condition-  
level decoding accuracy on 500-3000 ms. To investigate the  
time course of these correlations, Spearman’s Rho was calcu-  
lated at each time point. For condition-level alpha decoding,  
we investigated correlation between memory and decoding  
accuracy on 1,000-2,000 ms, the same time window reported  
in Fellner et al. (2020).

In item-level time-domain decoding, we investigated the  
correlations between decoding accuracy and absolute memory  
score of the same condition, on 0-500 ms and 500-3000 ms,  
respectively. To link item-level decoding with condition level  
inhibitory control theta power change, we calculated correla-  
tion between decoding accuracy difference between Think and  
No-Think on 420-600 ms, and theta power difference between  
Think and No-Think on 200-400 ms.

In the High- vs. Low-Suppression Grouping correlation, we  
calculated correlation between decoding accuracy on 300-680  
ms and No-Think minus Baseline Detail memory score, to be  
consistent with the grouping measure.

**High- vs. Low-Suppression Grouping.** We divided 40 participants  
into High- vs. Low-Suppression Groups, with 20 participants  
in each group based on the median split of No-Think-minus-  
Baseline Detail scores ranking. We used Detail because it  
captured both variability and suppression effects to a greater  
extent than did Identification (limited variability since it was  
a dichotomous measure) and Gist (did not show suppression  
effect). Pre-TNT learning was not different between Think  
and No-Think in either group ( $p > .116$ ).

#### Quantification and Statistical Analysis.

**Behavioral Analyses.** We conducted separate one-way ANOVAs  
with three within-subject conditions (Think vs. No-Think  
vs. Baseline) on the percentage of Identification, Gist, and  
Details. We then examined the suppression-induced forgetting  
effect by conducting planned pairwise t-test between No-think  
and Baseline, with a negative difference (i.e., No-Think mi-  
nus Baseline) indicating below-baseline, suppression-induced  
forgetting.

We report findings with  $p < .05$  as significant. Within-  
subject analyses of variance (ANOVAs) are reported with  
Greenhouse-Geisser corrected  $p$ -values whenever the assump-  
tion of sphericity was violated. We report Cohen’s  $d_z$  as effect  
size given our within-subject design (Lakens, 2013).

**Condition-/Item-level Decoding with Time Domain EEG.** Following  
the statistical analysis procedure (Bae & Luck, 2018), decoding  
accuracy at each time point (on 0-3000 ms) was compared to  
chance level by one-tailed paired t-test. Multiple comparisons  
were controlled by non-parametric cluster-based Monte-Carlo  
procedure. Specifically, a null distribution was constructed by  
assigning trial level classification results to random classes (as  
if the classifier has no knowledge of actual information), and  
then timepoint-by-timepoint t-tests were performed to obtain  
a maximum summed t-value of continuous significant time

908 cluster, which then repeated for 1,000 times. The resulting null  
909 distribution contained 1,000 summed t-values, which would  
910 be the distribution of the cluster summed ts when there is  
911 no true difference between decoding results and chance level.  
912 Both the cluster  $\alpha$  and the  $\alpha$  to obtain critical values from the  
913 permutation null distribution were set at 0.05 (on the positive  
914 tail, one-tail against chance).

915 The between-condition comparison of decoding accuracy  
916 along time were similar, except that the null distribution was  
917 constructed by randomly assigning condition labels to trial  
918 level classification results with two-tail repeated measure t-test  
919 and clusters were obtained on positive/negative tails, respec-  
920 tively. Thus, the critical values from the permutation null  
921 distribution were at 2.5% on the negative clusters null distri-  
922 bution and 97.5% on the positive clusters null distribution.

923 **Channel Searchlight Decoding.** We compared channel searchlight  
924 topographies between item-level decoding in Think and No-  
925 think with a two-tailed paired-sample t test at each channel.  
926 The multiple comparisons were controlled by cluster correction  
927 of channel neighbour clusters in Fieldtrip (Oostenveld et al.,  
928 2011). The neighborhood was defined as in the channel search-  
929 light analysis. Cluster  $\alpha$  was set at 0.05. Observed clusters  
930 were compared to null distribution on positive/negative tails  
931 respectively.

932 **Condition-/Item-level Decoding with Time-Frequency Domain EEG.**  
933 The statistical analyses for time-frequency domain decoding  
934 were similar to those of time domain decoding, except that  
935 here clusters were calculated in a 2-D matrix instead of on a  
936 1-D time axis, and the cluster  $\alpha$  was set at 0.05. Also, observed  
937 clusters were compared to the null distribution clusters of the  
938 same rankings. The statistical comparison of a single time-  
939 frequency decoding was performed against chance level (one-  
940 tailed), and that of the difference between two time-frequency  
941 decoding was performed against 0 (two-tailed). Theta (4-8 Hz)  
942 and alpha (9-12 Hz) decoding were assessed after averaging  
943 across the corresponding frequency bin.

944 **Time Frequency Analyses.** Early theta power at each electrode  
945 was compared between No-Think and Perceptual Baseline  
946 after averaging on 200-400 ms across 4 to 8 Hz, and then  
947 cluster corrected according to electrode positions in Fieldtrip  
948 (Oostenveld et al., 2011). The suppression-associated reduction  
949 of theta and alpha power on later time window was examined  
950 by averaging on 500-3000 ms across 4-8 Hz (theta) and 9-  
951 12 Hz (alpha), and then compared between No-Think and  
952 Think/Perceptual Baseline with neighbour cluster correction  
953 in Fieldtrip. The channel neighbours were defined in the same  
954 way as in channel searchlight analysis.

955 **Correlation Analyses.** The cluster correction for correlation time  
956 course was performed: we first transformed Spearman's Rho  
957 back to t-values to obtain the observed time-course clustered  
958 t-values and a null distribution. The null distribution was  
959 obtained by randomizing labels of the two variables of inter-  
960 est before calculating the Spearman's Rho and corresponding  
961 t-value. The cluster alpha was set as 0.05, and the observed  
962 clusters were calculated for positive and negative clusters re-  
963 spectively. The critical values of null distribution were at the  
964 2.5% on both tails. The comparison between 2 correlation co-  
965 efficients was conducted through a two-sided z test controlling  
966 for dependence (Lenhard & Lenhard, 2014).

**High- vs. Low-Suppression Groups Comparison.** Decoding accuracy  
967 at each time point on 0-3000 ms was compared between High-  
968 and Low suppression groups using two-tail independent t-test.  
969 The null distribution was constructed by randomly assigning  
970 group labels to each subject before by-timepoint t-test, to  
971 obtain the max summed-t of continuous significant time cluster  
972 when group labels are randomized, which repeated for 10,000  
973 times. The resulting 10,000 summed-t values would be the null  
974 distribution when no true difference exists between the two  
975 groups. Critical values from the permutation null distribution  
976 were at 2.5% on the negative clusters null distribution and  
977 97.5% on the positive clusters null distribution (two-tail,  $\alpha$   
978 = 0.05).  
979

980 **References**

- 981 Anderson, M. C., & Green, C. (2001). Suppressing unwanted  
982 memories by executive control. *Nature*, *410*(6826), 366–  
983 369.
- 984 Anderson, M. C., & Hanslmayr, S. (2014). Neural mechanisms  
985 of motivated forgetting. *Trends in Cognitive Sciences*,  
986 *18*(6), 279–292.
- 987 Anderson, M. C., & Hulbert, J. C. (2020). Active forget-  
988 ting: Adaptation of memory by prefrontal control. *Annual*  
989 *Review of Psychology*, *72*.
- 990 Anderson, M. C., Ochsner, K. N., Kuhl, B., Cooper, J., Robert-  
991 son, E., Gabrieli, S. W., Glover, G. H., & Gabrieli, J. D.  
992 (2004). Neural systems underlying the suppression of un-  
993 wanted memories. *Science*, *303*(5655), 232–235.
- 994 Bae, G.-Y., & Luck, S. J. (2018). Dissociable decoding of spa-  
995 tial attention and working memory from EEG oscillations  
996 and sustained potentials. *Journal of Neuroscience*, *38*(2),  
997 409–422.
- 998 Bastos, A. M., Vezoli, J., Bosman, C. A., Schoffelen, J.-M.,  
999 Oostenveld, R., Dowdall, J. R., De Weerd, P., Kennedy,  
1000 H., & Fries, P. (2015). Visual areas exert feedforward and  
1001 feedback influences through distinct frequency channels.  
1002 *Neuron*, *85*(2), 390–401.
- 1003 Bäuml, K.-H., Hanslmayr, S., Pastötter, B., & Klimesch, W.  
1004 (2008). Oscillatory correlates of intentional updating in  
1005 episodic memory. *NeuroImage*, *41*(2), 596–604.
- 1006 Benoit, R. G., Hulbert, J. C., Huddleston, E., & Anderson, M.  
1007 C. (2015). Adaptive top-down suppression of hippocam-  
1008 pal activity and the purging of intrusive memories from  
1009 consciousness. *Journal of Cognitive Neuroscience*, *27*(1),  
1010 96–111.
- 1011 Bergström, Z. M., Fockert, J. W. de, & Richardson-Klavehn, A.  
1012 (2009). ERP and behavioural evidence for direct suppres-  
1013 sion of unwanted memories. *NeuroImage*, *48*(4), 726–737.
- 1014 Catarino, A., Küpper, C. S., Werner-Seidler, A., Dalgleish, T.,  
1015 & Anderson, M. C. (2015). Failing to forget: Inhibitory-  
1016 control deficits compromise memory suppression in post-  
1017 traumatic stress disorder. *Psychological Science*, *26*(5),  
1018 604–616.
- 1019 Cavanagh, J. F., & Frank, M. J. (2014). Frontal theta as  
1020 a mechanism for cognitive control. *Trends in Cognitive*  
1021 *Sciences*, *18*(8), 414–421.
- 1022 Colgin, L. L. (2013). Mechanisms and functions of theta  
1023 rhythms. *Annual Review of Neuroscience*, *36*, 295–312.
- 1024 Colgin, L. L. (2016). Rhythms of the hippocampal network.  
1025 *Nature Reviews Neuroscience*, *17*(4), 239–249.
- 1026 Crespo-García, M., Wang, Y., Jiang, M., Anderson, M., &  
1027 Lei, X. (2021). Anterior cingulate cortex signals the need  
1028 to control intrusive thoughts during motivated forgetting.  
1029 *bioRxiv*.
- 1030 Delorme, A., & Makeig, S. (2004). EEGLAB: An open source  
1031 toolbox for analysis of single-trial EEG dynamics including  
1032 independent component analysis. *Journal of Neuroscience*  
1033 *Methods*, *134*(1), 9–21.
- 1034 Depue, B. E., Curran, T., & Banich, M. T. (2007). Prefrontal  
1035 regions orchestrate suppression of emotional memories via  
1036 a two-phase process. *Science*, *317*(5835), 215–219.
- 1037 Engen, H. G., & Anderson, M. C. (2018). Memory control: A  
1038 fundamental mechanism of emotion regulation. *Trends in*  
1039 *Cognitive Sciences*, *22*(11), 982–995.
- 1040 Fellner, M.-C., Waldhauser, G. T., & Axmacher, N. (2020).  
Tracking selective rehearsal and active inhibition of memory  
traces in directed forgetting. *Current Biology*, *30*(13), 2638–  
2644. e4.
- Gagnepain, P., Henson, R. N., & Anderson, M. C. (2014).  
Suppressing unwanted memories reduces their unconscious  
influence via targeted cortical inhibition. *Proceedings of*  
*the National Academy of Sciences*, *111*(13), E1310–E1319.
- Gagnepain, P., Hulbert, J., & Anderson, M. C. (2017). Parallel  
regulation of memory and emotion supports the suppression  
of intrusive memories. *Journal of Neuroscience*, *37*(27),  
6423–6441.
- Hanslmayr, S., Volberg, G., Wimber, M., Oehler, N., Staudigl,  
T., Hartmann, T., Raabe, M., Greenlee, M. W., & Bäuml,  
K.-H. T. (2012). Prefrontally driven downregulation of neu-  
ral synchrony mediates goal-directed forgetting. *Journal*  
*of Neuroscience*, *32*(42), 14742–14751.
- Hellerstedt, R., Johansson, M., & Anderson, M. C. (2016).  
Tracking the intrusion of unwanted memories into aware-  
ness with event-related potentials. *Neuropsychologia*, *89*,  
510–523.
- Hu, X., Bergström, Z. M., Bodenhausen, G. V., & Rosenfeld,  
J. P. (2015). Suppressing unwanted autobiographical mem-  
ories reduces their automatic influences: Evidence from  
electrophysiology and an implicit autobiographical memory  
test. *Psychological Science*, *26*(7), 1098–1106.
- Hu, X., Bergström, Z. M., Gagnepain, P., & Anderson, M.  
C. (2017). Suppressing unwanted memories reduces their  
unintended influences. *Current Directions in Psychological*  
*Science*, *26*(2), 197–206.
- Jensen, O., Gelfand, J., Kounios, J., & Lisman, J. E. (2002).  
Oscillations in the alpha band (9–12 hz) increase with  
memory load during retention in a short-term memory  
task. *Cerebral Cortex*, *12*(8), 877–882.
- Küpper, C. S., Benoit, R. G., Dalgleish, T., & Anderson, M. C.  
(2014). Direct suppression as a mechanism for controlling  
unpleasant memories in daily life. *Journal of Experimental*  
*Psychology: General*, *143*(4), 1443.
- Lakens, D. (2013). Calculating and reporting effect sizes to  
facilitate cumulative science: A practical primer for t-tests  
and ANOVAs. *Frontiers in Psychology*, *4*, 863.
- Lavenex, P., & Amaral, D. G. (2000). Hippocampal-  
neocortical interaction: A hierarchy of associativity. *Hip-*  
*podampus*, *10*(4), 420–430.
- Lenhard, W., & Lenhard, A. (2014). Hypothesis tests for com-  
paring correlations [Journal Article]. *Bibergau, Germany:*  
*Psychometrica*.
- Lopez-Calderon, J., & Luck, S. J. (2014). ERPLAB: An open-  
source toolbox for the analysis of event-related potentials.  
*Frontiers in Human Neuroscience*, *8*, 213.
- Mary, A., Dayan, J., Leone, G., Postel, C., Fraise, F., Malle,  
C., Vallée, T., Klein-Peschanski, C., Viader, F., & De la  
Sayette, V. (2020). Resilience after trauma: The role of  
memory suppression. *Science*, *367*(6479).
- Nigbur, R., Ivanova, G., & Stürmer, B. (2011). Theta power  
as a marker for cognitive interference [Journal Article].  
*Clinical Neurophysiology*, *122*(11), 2185–2194.
- Oostenveld, R., Fries, P., Maris, E., & Schoffelen, J.-M. (2011).  
FieldTrip: Open source software for advanced analysis of  
MEG, EEG, and invasive electrophysiological data. *Com-*  
*putational Intelligence and Neuroscience*, *2011*.
- Staresina, B. P., Reber, T. P., Niediek, J., Boström, J., Elger,

- 1102 C. E., & Mormann, F. (2019). Recollection in the human  
1103 hippocampal-entorhinal cell circuitry. *Nature Communica-*  
1104 *tions*, *10*(1), 1–11.
- 1105 Staesina, B. P., & Wimber, M. (2019). A neural chronometry  
1106 of memory recall. *Trends in Cognitive Sciences*, *23*(12),  
1107 1071–1085.
- 1108 Ter Wal, M., Linde-Domingo, J., Lifanov, J., Roux, F., Koli-  
1109 bius, L. D., Gollwitzer, S., Lang, J., Hamer, H., Rollings,  
1110 D., & Sawlani, V. (2021). Theta rhythmicity governs  
1111 human behavior and hippocampal signals during memory-  
1112 dependent tasks. *Nature Communications*, *12*(1), 1–15.
- 1113 Treder, M. S. (2020). MVPA-light: A classification and re-  
1114 gression toolbox for multi-dimensional data. *Frontiers in*  
1115 *Neuroscience*, *14*, 289.
- 1116 Treder, M. S., Charest, I., Michelmann, S., Martín-Buro, M.  
1117 C., Roux, F., Carceller-Benito, F., Ugalde-Canitrot, A.,  
1118 Rollings, D. T., Sawlani, V., Chelvarajah, R., Wimber, M.,  
1119 Hanslmayr, S., & Staesina, B. P. (2021). The hippocam-  
1120 pus as the switchboard between perception and memory.  
1121 *Proceedings of the National Academy of Sciences*, *118*(50),  
1122 e2114171118.
- 1123 van Schie, K., & Anderson, M. C. (2017). Successfully con-  
1124 trolling intrusive memories is harder when control must be  
1125 sustained. *Memory*, *25*(9), 1201–1216.
- 1126 Waldhauser, G. T., Bäuml, K.-H. T., & Hanslmayr, S. (2015).  
1127 Brain oscillations mediate successful suppression of un-  
1128 wanted memories. *Cerebral Cortex*, *25*(11), 4180–4190.
- 1129 Wimber, M., Alink, A., Charest, I., Kriegeskorte, N., & Ander-  
1130 son, M. C. (2015). Retrieval induces adaptive forgetting  
1131 of competing memories via cortical pattern suppression.  
1132 *Nature Neuroscience*, *18*(4), 582–589.
- 1133 Wolff, M. J., Jochim, J., Akyürek, E. G., & Stokes, M.  
1134 G. (2017). Dynamic hidden states underlying working-  
1135 memory-guided behavior. *Nature Neuroscience*, *20*(6),  
1136 864–871.
- 1137 Xie, S., Kaiser, D., & Cichy, R. M. (2020). Visual imagery  
1138 and perception share neural representations in the alpha  
1139 frequency band. *Current Biology*, *30*(13), 2621–2627. e5.
- 1140 Yaffe, R. B., Kerr, M. S., Damera, S., Sarma, S. V., Inati, S.  
1141 K., & Zaghoul, K. A. (2014). Reinstatement of distributed  
1142 cortical oscillations occurs with precise spatiotemporal dy-  
1143 namics during successful memory retrieval. *Proceedings of*  
1144 *the National Academy of Sciences*, *111*(52), 18727–18732.
- 1145 Zhang, D., Xie, H., Liu, Y., & Luo, Y. (2016). Neural corre-  
1146 lates underlying impaired memory facilitation and suppres-  
1147 sion of negative material in depression. *Scientific Reports*,  
1148 *6*(1), 1–10.